International Journal of Computer Applications Technology and Research
Volume 14–Issue 10, 35 – 39, 2025, ISSN:-2319–8656
DOI:10.7753/IJCATR1410.1008

Design and Analysis of a Constant Temperature Difference Thermal Distributed Flow Sensor Based on MEMS Technology

Yuexiang Wang
Chengdu University of Information Technology
College of Communication Engineering
ChengDu, China

Jing Zeng
Chengdu University of Information Technology
College of Electronic Engineering
ChengDu, China

Bin Wen*
Chengdu University of Information Technology
College of Communication Engineering
ChengDu, China

Abstract: Based on the development of MEMS technology, this paper studies a constant temperature difference (CTD) thermal distributed flow sensor known for its low startup flow, high accuracy, and repeatability. A theoretical model with insulated microgrooves and cavities is established, confirming that stabilizing the temperature difference between the heating resistor and the ambient environment improves sensor accuracy. According to Thomas's theory, flow rate is derived from the temperature difference detected by upstream and downstream sensing resistors. A dedicated CTD circuit is designed and tested, showing excellent linearity ($R^2 \geq 0.9954$) and low temperature-dependent error (<0.11%), effectively maintaining the set temperature difference within 0–50°C.

Keywords: MEMS; Thermal Flow Sensor; Constant Temperature Difference; Thermal Distributed; Modeling;

1. INTRODUCTION

The development of Micro-Electro-Mechanical Systems (MEMS) and the growing need for accurate flow measurement have led to the widespread application of MEMS-based thermal flow sensors. These sensors are valued for their low startup flow, minimal pressure loss, high precision, and excellent repeatability, finding uses in industrial control, biomedical fields, chemical synthesis, and biochemistry [1].

Thermal loss type sensors, designed based on King's law and driven by constant temperature difference (CTD) or constant power (CP) modes, suffer from long response times, unstable zero points, low accuracy at low flow rates, and significant influence from fluid temperature [2].

Current research predominantly focuses on thermal loss type flow meters based on CTD or CP modes [3-7]. Studies on CTD thermal distributed flow meters are relatively scarce [8, 9]. Given their advantages of low startup flow, small pressure loss, and good repeatability, research on this type of sensor is necessary. Therefore, this paper investigates the thermal distributed flow meter operating in constant temperature difference mode.

This paper establishes a theoretical model for a thermal distributed flow sensor with insulating microgrooves and a cavity. Model analysis shows that reducing the fluctuation in the temperature difference between the ambient environment and the heating resistor can enhance the stability of the sensor's temperature field distribution, thereby improving the accuracy of the flow meter.

2. PRINCIPLE OF FLOWMETER

International Journal of Computer Applications Technology and Research
Volume 14–Issue 10, 35 – 39, 2025, ISSN:-2319–8656
DOI:10.7753/IJCATR1410.1008

2.1 Theoretical Model of Sensor

To describe the key characteristics of the flow sensor, the lumped parameter method is adopted instead of solving the nonlinear coupled partial differential equations of fluid dynamics and heat transfer. Assuming the temperature distribution in the y-direction for the fluid and film within a square channel of height hc is piecewise linear, and the temperature distribution perpendicular to the x-y plane (Z-direction) is identical to that in the x-y plane, the 3D heat transfer analysis is simplified to a 1D analysis along the x-y plane.

The 1D structural model is divided into four regions based on thermal conductivity (W·m⁻¹·K⁻¹): k_f (fluid flow zone), k_{f_1} (insulated microgroove zone), k_s (composite film zone), and k_{f_2} (insulated cavity zone), as shown in Figure 1.

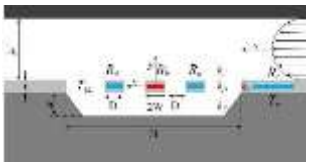

Figure 1. Modeling of thermal flow sensors

Parameters t、h、L、W、D、D_1 represent composite film thickness, insulated cavity depth, half-length of the insulated cavity, half-width of the heating resistor, width of the insulated microgroove, and half-width of the temperature-sensing resistor, respectively (units: m). The temperature distribution in the y-direction and the control volume Δx×y×1 for heat flux analysis are shown in Figure 2, where Q is the heat flux (W), superscripts cond and conv denote heat conduction and convection, and subscripts f, f₁, s, f₂ denote the respective zones.

Figure 2. The control volume for heat flux analysis

Under steady-state flow conditions, aside from the heating resistor region, the incoming and outgoing convective and conductive heat fluxes within the control volume Δx×y×1 are equal[10].

$$Q^{cond}_{f,x} + Q^{conv}_{f,x} + Q^{cond}_{f_1,x} + Q^{cond}_{f2,x} = Q^{cond}_{f,y} + Q^{cond}_{f2,y} \quad (1)$$

$$Q^{cond}_{f,x} + Q^{conv}_{f,x} + Q^{cond}_{s,x} + Q^{cond}_{f2,x} = Q^{cond}_{f,y} + Q^{cond}_{f2,y} \quad (2)$$

The incoming and outgoing conductive heat fluxes can be calculated.

$$Q^{cond}_{f,x} = \frac{1}{2} k_f \frac{d^2T(x)}{dx^2} \Delta x \delta_{t,x} \quad (3)$$

$$Q^{conv}_{f,x} = -\rho C_P v \frac{dT(x)}{dx} \left(\frac{\delta_{t,x}}{h_c} - \frac{\delta^2_{t,x}}{2h_c^2}\right) \Delta x \quad (4)$$

$$Q^{cond}_{f_1,x} = k_{f1} \frac{d^2T(x)}{dx^2} \Delta x t \quad (5)$$

$$Q^{cond}_{s,x} = k_s \frac{d^2T(x)}{dx^2} \Delta x t \quad (6)$$

$$Q^{cond}_{f_2,x} = \frac{1}{2} k_{f_2} \frac{d^2T(x)}{dx^2} \Delta x h \quad (7)$$

$$Q^{cond}_{f,y} = k_f \frac{T(x)}{\delta_{t,x}} \Delta x \quad (8)$$

$$Q^{cond}_{f2,y} = k_{f2} \frac{T(x)}{h} \Delta x \quad (9)$$

Parameters ρ, C_P, and v represent the fluid's density (kg·m⁻³), constant-pressure specific heat capacity (J·kg⁻¹·K⁻¹), and flow velocity (m·s⁻¹), respectively. δ_(t,x) is the thermal boundary layer thickness (m).

On the fluid-solid coupling interface, ignoring processes like radiation and ablation phase change, the energy continuity equation is satisfied, meaning temperature and heat flux density are equal, thus $Q^{cond}_{f1,x} = Q^{cond}_{s,x}$. Equating equations (1) and (2) and substituting equation (3) yields a second-order homogeneous differential equation concerning the one-dimensional temperature distribution T(x) of the

sensor.[11]

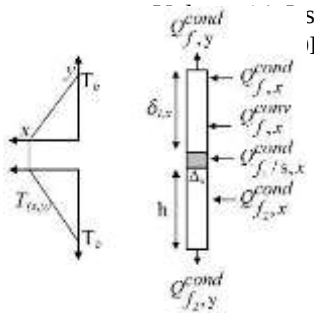

$$\left(\frac{1}{2}k_f\delta_{t,x} + k_{f_1}t + \frac{1}{2}k_{f_2}h\right)\frac{d^2T(x)}{dx^2} - \rho C_P v\left(\frac{\delta_{t,x}^2}{h_c} - \frac{\delta_{t,x}^3}{2h_c^2}\right)\frac{dT(x)}{dx} - \left(\frac{k_f}{\delta_{t,x}} + \frac{k_{f_2}}{h}\right)T(x) = 0 \quad (10)$$

This differential equation cannot be solved analytically

International Journal of Computer Applications Technology and Research
Volume 14–Issue 10, 35 – 39, 2025, ISSN:-2319–8656
DOI:10.7753/IJCATR1410.1008

without analyzing the thermal boundary layer $\delta_{t,x}$. Wei Xu's research provided an explicit function expression for the thermal boundary layer.[12]

$$\delta_{t,x} = h_c\left(\frac{15\ x+L}{4Re_cPr\ h_c}\right)^{\frac{1}{3}} - L < x < L \qquad (11)$$

The channel Reynolds number is defined as $Re_c = \rho v h / \mu$ *, where* μ *is the dynamic viscosity of the fluid* ($m^2 \cdot s^{-1}$). $P_r = \rho C_p^f \mu_f / k_f$. *nn rractice, the thermal boundary layer develors at different rates urstream and downstream. nntroducing urstream (*$\delta_{t,u}$) and downstream ($\delta_{t,d}$) average boundary layers allows for separate analysis.

$$\delta_{t,d} = \frac{\int_0^L \delta_{t,x}\, dx}{L} = 1.77\left(\frac{c}{Re_cPr}\right)^{\frac{1}{2}} \qquad (12)$$

$$\delta_{t,u} = \frac{\int_{-L}^{0} \delta_{t,x}\, dx}{L} = 1.17\left(\frac{c}{Re_cPr}\right)^{\frac{1}{2}} \qquad (13)$$

herein, $A_d = \frac{1}{2}k_f\delta_{t,d} + k_{f_1}t + \frac{1}{2}k_{f_2}h$, $A_u = \frac{1}{2}k_f\delta_{t,u} + k_{f_1}t + \frac{1}{2}k_{f_2}h$, $B = -\rho C_P v\left(\frac{\delta_{t,x}}{h_c} - \frac{\delta_{t,x}^2}{2h_c^2}\right)$, $C = -\left(\frac{k_f}{\delta_{t,x}} + \frac{k_{f_2}}{h}\right)$。

The sensor features a Si_3N_4-SiO_2-Si_3N_4 composite dielectric film structure. Si_3N_4 has a thermal conductivity of about 150 $W \cdot m^{-1} \cdot K^{-1}$, making it a good thermal conductor. Thus, the temperature at both ends of the sensor equals the ambient temperature T_e, and the temperature in the heating resistor region is T_h (°C). Applying the boundary conditions $T(-L) = T_e$, $T(-W) = T_h$; $T(L) = T_e$, $T(W) = T_h$,the analytical solution for the temperature distribution T(x) along the flow direction (x-direction) is finally determined.

$$\begin{cases} T(x) = \frac{T_h(e^{xr_{u1}-Lr_{u2}} - e^{xr_{u2}-Lr_{u1}}) + T_e(e^{xr_{u2}-Wr_{u1}} - e^{xr_{u1}-Wr_{u2}})}{e^{-Wr_{u1}-Lr_{u2}} - e^{-Wr_{u2}-Lr_{u1}}}; & -L \le x \le -W \\ T(x) = T_h; & -W \le x \le W \\ T(x) = \frac{T_h(e^{xr_{d1}+Lr_{d2}} - e^{xr_{d2}+Lr_{d1}}) + T_e(e^{xr_{d2}+Wr_{d1}} - e^{xr_{d1}+Wr_{d2}})}{e^{Wr_{d1}+Lr_{d2}} - e^{Wr_{d2}+Lr_{d1}}}; & W \le x \le L \end{cases} \qquad (14)$$

Herein, r_d1、r_d2、r_u1、r_u2are the characteristic roots of differential equation (4): $r_{d1} = \frac{-B-\sqrt{B^2-4AC}}{2A_d}$, $r_{d2} = \frac{-B+\sqrt{B^2-4AC}}{2A_d}$, $r_{u1} = \frac{-B-\sqrt{B^2-4AC}}{2A_u}$, $r_{u2} = \frac{-B+\sqrt{B^2-4AC}}{2A_u}$。 Furthermore, considering that the upstream and downstream temperature-sensing resistors are not point sensors, the average temperatures at the upstream and downstream resistors are: $T_d = \frac{\int_{W+D}^{W+D+D_1} T(x)dx}{D_1}$, $T_u = \frac{\int_{-W-D-D1}^{-W-D} T(x)dx}{D_1}$. The temperature difference between the upstream and downstream resistors is obtained as $\Delta T = T_d - T_u$;

2.2 Measurement Principle

heat from the upstream part to the downstream, causing a temperature difference ΔT (°C) between upstream and downstream, as shown by the red line. The magnitude of this difference reflects the fluid flow rate, ΔT = f(m). When the fluid velocity is too high, ΔT approaches zero; thus, thermal distributed flow sensors are used for low to medium flow measurements. The gas mass flow rate q_m can be expressed as indicated.

$$q_m = K\frac{A}{C_p}\Delta T \qquad (15)$$

$C_p$is the constant-rressure srecific heat caracity of the fluid (J/(kg·K)); A is the thermal conduction coefficient

The flow meter works by maintaining a constant temperature difference (T_h) between the heating resistor (heat source) temperatureT_w and the ambient

International Journal of Computer Applications Technology and Research
Volume 14–Issue 10, 35 – 39, 2025, ISSN:-2319–8656
DOI:10.7753/IJCATR1410.1008

temperature T_e When no fluid flows, the temperature distribution on both sides of the heating resistor is symmetrical, as shown by the blue line in Figure 3. When fluid flows at a constant velocity, it transports

(W/(m·K)); K is the meter coefficient

From the one-dimensional heat transfer model, when factors like gas type, sensor dimensions, ambient temperature, temperature difference between heat source and environment, and pipeline characteristics are determined, the relationship between mass flow rate q_v and sensor thermal output ΔT is obtained: $\Delta T = T(D+W) - T(-D-W) = f_{(q_v)}$. The temperature difference T_h crucially affects the sensor's temperature

International Journal of Computer Applications Technology and Research
Volume 14–Issue 10, 35 – 39, 2025, ISSN:-2319–8656
DOI:10.7753/IJCATR1410.1008

distribution, which directly influences the stability of the temperatures at the upstream and downstream sensing resistors. Therefore, maintaining a constant T_h is essential for output stability and accuracy. Consequently, a CTD maintenance circuit was designed for this study, its principle shown in Figure 4.

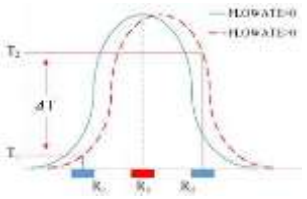

Figure 3. Schematic diagram of thermal distributed flow sensor measurement principle

The CTD circuit uses a Wheatstone bridge composed of R_1、R_r、R_e、R_h、R_4、R_5. The ambient temperature sensing resistor R_e and heating resistor R_h are on two arms of the bridge. R_2、R_3 are comparator input current-limiting resistors, C_1 is a buffer capacitor, C_2 is a transistor switch acceleration capacitor, R_7 is a comparator output pull-up resistor, R_r is a digital potentiometer communicating with the MCU via SPI to program the voltage at the comparator's positive input, controlling the operating voltage of R_h and thus the temperature difference.

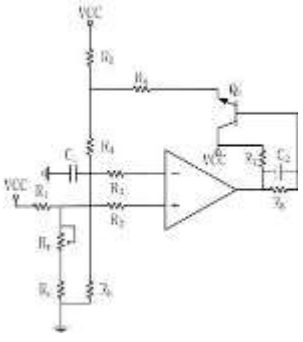

Figure 4. Constant temperature difference circuit

When the fluid temperature changes, the constant temperature difference (CTD) circuit compensates by supplying a corresponding current to the heating resistor via the Wheatstone bridge, thereby controlling and maintaining a constant temperature difference between the heating resistor and the gas temperature. However, it should be noted that the resistors in the Wheatstone bridge of the CTD circuit must satisfy the following formula:

$$(R_4 + R_5) * R_{e_0} = R_{h_0} * R_1 \quad (16)$$

Only under this condition can the constant temperature difference (CTD) circuit maintain a stable temperature difference. Herein, R_{h_0} *is the resistance value of the heating resistor* R_h *at 0°C, and* R_{e_0} is the resistance value of the ambient resistor R_e at 0°C, with the unit for both being Ω (Ohms).

The sensor measurement circuit is shown in Figure 5. Resistors R_9、R_{10}、R_u、R_d form a Wheatstone bridge (R_9=R_{10}，R_u=R_d). When flow is zero, the bridge output is zero. When flow changes, the resistances of the upstream and downstream temperature-sensing resistors change, and the bridge outputs a voltage corresponding to the flow rate. This analog voltage signal is converted to digital via an ADC and sent to the MCU via SPI for flow calculation. High-precision, low-temperature-drift chip resistors are used on the Wheatstone bridge to minimize effects from resistor tolerance and temperature drift.

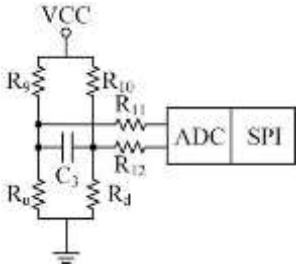

Figure 5. Measurement circuit schematic diagram

3. SYSTEM TESTING

Based on the sensor calibration results, the linear functional relationship between the ambient resistor, heating resistor, and temperature is known. The heating temperature was calculated from the voltage across the platinum resistor. In the CTD circuit, the fixed resistor values were: R_1=6800Ω, R_5=1330Ω, R_4=30Ω. The digital potentiometer R_r was varied from 0-3300 Ω to control the gas temperature from 0-50°C, and the voltage change across the heating resistor was measured and converted to heating resistor temperature values. The test results are shown in Figure 6.

Figure 6.Test results of the constant temperature difference circuit

REFERENCES

[1] Xu W, Ma S, Wang X, et al. A CMOS-MEMS thermoresistive micro calorimetric flow sensor with temperature compensation[J]. Journal of Microelectromechanical Systems, 2019, 28(5): 841-849.

[2] Xu W, Gao B, Ma S, et al. Low-cost temperature-compensated thermoresistive micro calorimetric flow sensor by using 0.35 μm CMOS MEMS technology[C]//2016 IEEE 29th International Conference on Micro Electro Mechanical Systems (MEMS). IEEE, 2016: 189-192.

[3] Nguyen N T. Micromachined flow sensors—A review[J]. Flow measurement and Instrumentation, 1997, 8(1): 7-16.

[4] Aleksic S O, Mitrovic N S, Lukovic M D, et al. Heat loss flowmeter for water based on thick film thermistors in power save regime[J]. IEEE Sensors Journal, 2020, 21(1): 199-206.

[5] Tong X, Hao B, Chen Z, et al. Thermal airflow sensor design and temperature compensation research based on the thermostatic method[J]. Sensor Review, 2022, 42(5): 568-575.

[6] Bernhardsgrütter R E, Hepp C J, Wöllenstein J, et al. Fluid-compensated thermal flow sensor: A combination of the 3ω-method and constant temperature anemometry[J]. Sensors and Actuators A: Physical, 2023, 350: 114116.

[7] Wang L, Zhu R, Li G. Temperature and strain compensation for flexible sensors based on thermosensation[J]. ACS applied materials & interfaces, 2019, 12(1): 1953-1961.

[8] Fan X, Hou L, Wu W, et al. Study on a low-disturbance and anti-interference dual-mode micro thermal flow sensor for heat-sensitive liquid[J]. Measurement, 2026, 257: 118641.

[9] Bekraoui A, Hadjadj A. Thermal flow sensor used for thermal mass flowmeter[J]. Microelectronics journal, 2020, 103: 104871.

[10] Wang J, Li X. Package-friendly piezoresistive pressure sensors with on-chip integrated packaging-stress-suppressed suspension (PS3) technology[J]. Journal of Micromechanics and Microengineering, 2013, 23(4): 045027.

[11] Sharifian A, Wells K. Performance assessment of ISO-5167 and symmetrical Venturi meters for measuring low Reynolds number turbulent incompressible isothermal flow[J]. International Journal of Thermofluids, 2024, 22: 100598.

[12] Fürjes P, Légrádi G, Dücső C, et al. Thermal characterisation of a direction dependent flow sensor[J]. Sensors and Actuators A: Physical, 2004, 115(2-3): 417-423.